Dosimetric characterization of a bi-directional micromultileaf collimator for stereotactic applications

M. Bucciolini,[a] S. Russo, F. Banci Buonamici, S. Pini, and P. Silli
Department of Clinical Physiopathology, Medical Physics Unit, University of Florence, Florence, Italy

(Received 3 December 2001; accepted for publication 21 April 2002; published 20 June 2002)

A 6 MV photon beam from Linac SL75-5 has been collimated with a new micromultileaf device that is able to shape the field in the two orthogonal directions with four banks of leaves. This is the first clinical installation of the collimator and in this paper the dosimetric characterization of the system is reported. The dosimetric parameters required by the treatment planning system used for the dose calculation in the patient are: tissue maximum ratios, output factors, transmission and leakage of the leaves, penumbra values. Ionization chambers, silicon diode, radiographic films, and LiF thermoluminescent dosimeters have been employed for measurements of absolute dose and beam dosimetric data. Measurements with different dosimeters supply results in reasonable agreement among them and consistent with data available in literature for other models of micromultileaf collimator; that permits the use of the measured parameters for clinical applications. The discrepancies between results obtained with the different detectors (around 2%) for the analyzed parameters can be considered an indication of the accuracy that can be reached by current stereotactic dosimetry. [DOI: 10.1118/1.1487423]

Key words: micromultileaf collimator, small field dosimetry, stereotactic radiotherapy

I. INTRODUCTION

The radiotherapic treatment procedures have been consistently upgraded in recent years, because of continuously developing technologies. In particular, the improvement affects some aspects, such as target definition, patient positioning, and beam delivery techniques, which are of main concern for stereotactic applications.

Sophisticated imaging equipment helps to define with extreme precision the target volume, the immobilization techniques allow the positioning of the patient during the treatment with always increasing accuracy, the accelerators are equipped with beam modifying devices able to realize dose distributions closely shaped on the target volume. All that explains the spread of conformal techniques, in particular those making use of stereotactic procedures. In this case a reference system is associated with the positioning and immobilization devices, which allows one to fix the beam isocenter at the center of the lesion. The same device, equipped with localization bars, is used during the imaging phase, allowing one to refer the structures of interest to the stereotactic coordinate system. During the planning phase of the treatment, the analysis of different modality images permits one to identify the target center in the stereotactic frame.

For the application of the technique to intracranial tumors, it is necessary to realize narrow irradiation fields, shaped on the targets, which are of small dimensions (4 mm–10 cm) and in case irregular. The required precision is greater than that achievable with traditional irradiation techniques. In order to reach this goal, at the Radiotherapy Department of the University of Florence, we are testing a micromultileaf collimator (μMLC) that fits on the head of the linear accelerator Elekta SL75-5. The Acculeaf device was installed by Alayna (Alayna Enterprises Corporation, Paris, France) in experimental phase. It consists of two levels of thin leaves, able to move along two orthogonal directions. The leaf width, projected to the isocenter, is a few millimeters. The exclusive feature of bi-directional leaf setting makes it possible to shape irregular small fields with great accuracy. Up to now such accuracy could not be reached either with the most usual multileaf collimators having leaves 1 cm wide, or with other commercial micromultileaf collimators having leaves moving only along one direction. The μMLC clinical implementation needs its dosimetric characterization with the 6 MV photon beam used for stereotactic radiotherapy. The measurements of small radiation fields raise specific dosimetric problems.[1–3] The steep dose gradients and the lack of lateral electronic equilibrium address the employment of high spatial resolution detectors, able to carry out, in such critical conditions,[4] the beam mapping and calibration. With this aim, the following detectors have been tested and compared: ionization chambers of different geometry, silicon stereotactic diode, thermoluminescent dosimeters, and radiographic films. The measured dosimetric parameters, input data for the calculation algorithm of the dose to the patient, are transmission under and between leaves, spatial distributions of the dose, penumbra, calibration factor in reference conditions and output factors. The calculation model, implemented on a dedicated commercial treatment planning system, is of semiempirical type and it predicts the beam output for the μMLC shaped fields by the area/perimeter formalism. The off-axis dose is evaluated by convolution of a flat distribution with a blurring function based on measured data. The aim of this work is the determination of the required parameters and the evaluation of the accuracy that can be achieved with the different detectors.

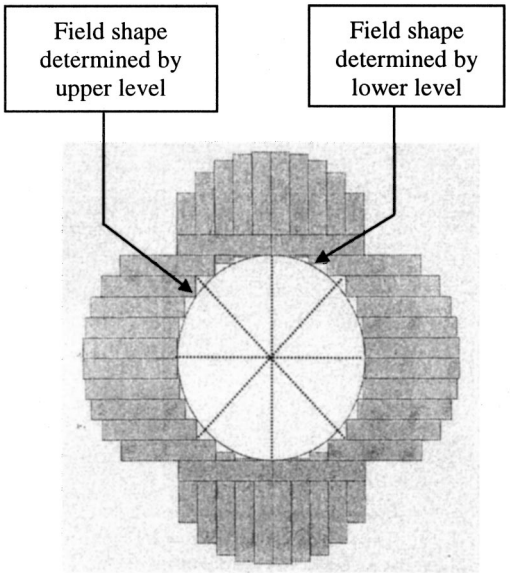

FIG. 1. Circular field shaped by the two levels of leaves of the μMLC. The circle is divided into eight sectors; each of them is defined by four leaves of either the upper or the lower level.

II. MATERIAL AND METHODS

A. Micromultileaf design

The Acculeaf micromultileaf collimator, produced by Alayna Enterprises Corp., and provided by Direx Systems srl, is mounted on a SL75-5 Elekta linear accelerator. It consists of 96 tungsten leaves (48 pairs) and singular motors move each of them. The leaves are settled on two levels, positioned at different distance from the source, and perpendicular to each other. The 14 inner pairs of each level are made of thinner leaves (physical width 2.1 mm). They form a fine resolution field of about 50 mm$\times$45 mm at the isocenter, due to the projected widths of about 3.6 mm, for the bank closer to the radiation source, and 3.2 mm for the farther away. The physical width of the 10 outer pairs is 3.6 mm. The maximum square field that can be defined at isocenter is 97 mm$\times$108 mm. Each leaf has a height of 37.5 mm and a physical length of 60 mm; its total travel is 88 mm at isocenter and the maximum shift beyond the center is 31 mm.

Due to the presence of two levels of leaves in this μMLC, it is possible to define an ''effective'' leaf width. It corresponds to the width that would be necessary, with a single level of leaves, to obtain the same exposed field as that generated by our four leaves banks, without intrusion into the target outline. In Fig. 1 the exposed field generated by the two levels of leaves for a circled shape is shown. The ''effective'' leaf width of the inner pairs is 2.6 mm at the isocenter, while for the leftover 10 pairs it is 4.5 mm.

Under each bank, two thin carbon bars (2 mm) are mounted orthogonal to the leaf movement direction in order to prevent any leaf bending.

Leaf motion and positioning are checked by a closed loop video guided system that utilizes four charge coupled device cameras, integrated in each leaf bank. The μMLC is 540 mm in outer diameter, 135 mm in height, and 28 kg in weight.

The μMLC is manually mounted on the linac with the gantry turned to 180°. The total mounting and initialization time is about 15 min. The system is interfaced by device control software to a PC controlling and visualizing leaf configuration.

B. Dosimetric tools

In this study the beam characterization measurements have been carried out with several detectors, which have different sensitivity and spatial resolution: Exradin T1, PTW PinPoint and Scanditronix RK thimble ionization chambers, Scanditronix *p*-type silicon stereotactic diode (SFD), TLD 100 microcubes, Kodak X-OMAT films.

The Exradin T1 chamber has a collecting volume of 0.05 cm^3, a cavity diameter of 4 mm, and a cavity length of 5.7 mm. Outer walls, collector, and guard material are tissue equivalent plastic A150. This detector has been calibrated by intercomparison with a Farmer cylindrical ionization chamber, whose calibration factor, in terms of dose to air, has been furnished by the National Reference Laboratory (ENEA, Casaccia). A ^{60}Co beam has been used for the intercomparison measurement.

The PTW Pin Point chamber has a measuring volume of 0.015 cm^3; the cavity is only 2 mm in diameter and 5 mm in length. Walls are made by PMMA and graphite, while the collector is made by steel. Its calibration factor is furnished by PTW in terms of dose to water.

The Scanditronix RK chamber is a cylindrical ionization chamber intended for measurements in water phantom. The air cavity has a volume of 0.12 cm^3, a diameter of 4 mm, and a length of 10 mm. Both the central collecting electrode and inner lining of the encapsulating Perspex cylinder are of graphite/epoxy material.

The stereotactic field detector (SFD-Scanditronix) is a *p*-type boron-doped silicon diode. The effective thickness of the sensitive volume is 0.06 mm and the diameter of the active area is 0.6 mm. The detector was pre-irradiated with 8 kGy of 20 MeV electrons; this means that further irradiations slowly affect the sensitivity.

The dimension of all the detectors are summarized in Table I.

The employed TLD 100 microcubes (LiF:Mg, Ti), acquired by Bicron®, have dimensions of $1\times1\times1$ mm^3. Their response to the irradiation (integral below the Glow Curve) has been measured with a Harshaw 2000 reader. The 100 samples used have been calibrated with the Farmer chamber in a broad 6 MV photon beam for dose ranging from 7 to 450 cGy. For each detector a specific sensitivity factor has been determined. The reading temperature rate is about 9 °C/s, the annealing procedure after reading consists in 1 h at 400 °C and 2 h at 100 °C in oven. With these operating procedures the global accuracy on the absorbed dose can be evaluated about 3%.

Film dosimetry measurements have been performed using the standard KOKAD X-OMAT XV2 film for therapy veri-

TABLE I. Geometrical features of the employed dosimeters.

Ionization chamber	Volume	Cavity length	Cavity diameter
PTW Pin Point	0.015 cc	5 mm	2 mm
Ionization chamber	Volume	Cavity length	Cavity diameter
Exradin T1	0.05 cc	5.7 mm	4 mm
Ionization chamber	Volume	Cavity length	Cavity diameter
Scanditronix RK	0.12 cc	10 mm	4 mm
Stereotactic diode	Volume	Active area	Sensitive volume
Scanditronix SFD	1.7×10^{-5} cc	diameter	thickness
		0.6 mm	60 μm
Microcubes	Volume	Area	Thickness
TLD 100	1 mm^3	1 mm^2	1 mm
Film	Pixel size	Laser scanning spot size	
Kodak X-OMAT XV2	100 μm	100 μm	

fication. The films have been calibrated in terms of dose-optical density relationship at the energy quality of interest (6 MV from Elekta SL75-5 linac). The resulting images have been digitalized with a Lumisys LS100 laser scanner.

C. Film calibration

The film calibration has been performed in two different situations, always keeping the source to film distance equal to 100 cm and the field equal to $5\times5\ cm^2$. In both cases doses ranged approximately from 1 cGy up to 100 cGy and depth was at 1.5 cm in PMMA or 4.2 cm in PMMA; no substantial differences were found between the two data sets. The absorbed dose has been measured with ionimetric method, employing as a reference a Farmer NE2571 ion chamber coupled to a Keithley 35040 electrometer.

The resulting images have been digitalized with a Lumisys LS100 film scanner and analyzed with a home-developed software. The calibration points have been interpolated with a sixth degree polynomial and the resulting function has been applied to the original images. Figures 2(a) and 2(b) show the calibration points with the fit curves overlaid, the first one represents the relationship between dose and pixel value, while the second one illustrates the inverse.

For accuracy verification, some sample points, not used for the calibration, have been measured. Out of the "fog" region the disagreement between calculated and measured points is within 5%. This result agrees with the published data for the accuracy of film dosimetry in the high energy range.[5–7]

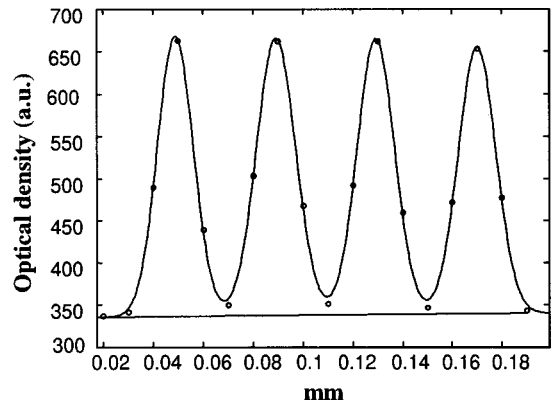

FIG. 3. Outer diameter profile reconstructed from the image of a bar pattern of 2.5 lp/mm. The profile has been fitted with four Gaussian curves having the parameters reported (1) $X_{med}=0.49$ mm, $\sigma=0.07$ mm; (2) $X_{med}=0.89$ mm, $\sigma=0.08$ mm; (3) $X_{med}=1.30$ mm, $\sigma=0.075$ mm; (4) $X_{med}=1.70$ mm, $\sigma=0.08$ mm.

The films have been digitalized with a pixel size of 100 μm, the spot size of the scanning laser is also 100 μm. The accuracy of the procedure for distance measurements has been evaluated using a standard bar pattern, with resolutions ranging from 2 to 6 lp/mm; the resulting OD profile has been investigated for the 2.5 lp/mm resolution. Gaussian profiles are expected with distances of 400 μm between adjacent maxims. The distance between a maximum and the following minimum is about 200 μm, as displayed in Fig. 3; this has been verified for both image axes. We assume 200 μm as uncertainty in distance evaluation.

D. Output factors

Output factors have been measured with the PTW Pin Point chamber for square fields from 1×1 to $10\times10\ cm^2$. The chamber has been placed at the isocenter in a water phantom at a depth from the surface of 1.5 and 5 cm. All the data have been normalized referring to the measurement with a $10\times10\ cm^2$ field shaped by the jaws, without the μMLC. The output factors have been estimated for two conventional jaw configurations: in the first case the conventional jaws were maintained to the $10\times10\ cm^2$ opening, in the latter they followed the μMLC aperture with a 2 mm margin for each jaw.

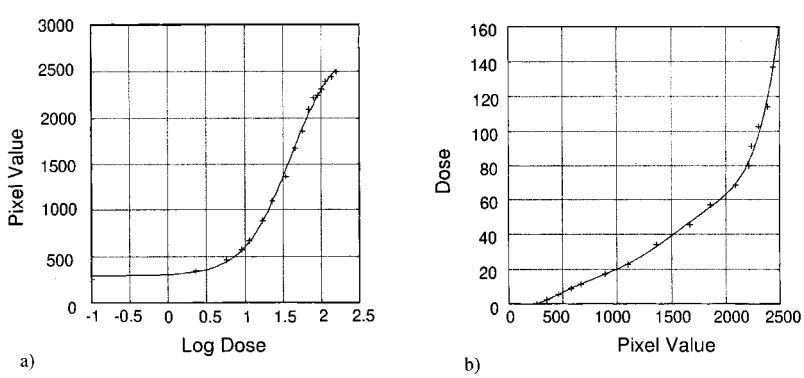

FIG. 2. Sensitometric curve for a 6 MV photon beam with a $5\times5\ cm^2$ field and a depth of 4.2 cm in PMMA: (a) relation between pixel value and dose, (b) calibration curve reversed. All doses in cGy.

Keeping the jaws open to $10\times10\ \mathrm{cm}^2$, output factors have been also evaluated with other different kinds of detectors: SFD diode, T1 and RK ionization chambers in water phantom, and TLD 100 microcubes in PMMA. Also smaller field dimensions (from $0.3\times0.3\ \mathrm{cm}^2$) have been investigated with SFD diode and LiF dosimeters.

E. Leakage and leaf transmission tests

Measurements of leaf leakage and transmission have been carried out using X-OMAT V films positioned at the isocenter, perpendicularly to the beam central axis in PMMA, at a water equivalent depth of 1.5 cm ($d_{\max}$). The experiments have been repeated positioning the Farmer chamber at 1.5 cm in water, at the isocenter.

In order to normalize all measurements, a $5\times5\ \mathrm{cm}^2$ field has been first investigated. It was obtained with conventional jaws and without μMLC. The dose on the central axis has been determined by delivering 50 MU.

The transmission under the jaws has been studied fully closing the jaws and shooting 1800 MU. The third configuration has been reached with the primary jaws set to $5\times5\ \mathrm{cm}^2$ and the μMLC leaves fully closed: with this setup the transmitted dose under the μMLC has been measured with 1800 MU.

The leaf closing happens at 3.1 mm from the center of the beam. The dose under each group of leafs (upper and lower) has been evaluated too, by shooting 400 MU.

F. Penumbra test

The behavior of the penumbra 20%–80% for square fields has been investigated measuring two orthogonal profiles in a plane perpendicular to the beam axis, at 1.5 and 5 cm depth in water. The size of the fields varied from 1 to 9 cm. Data have been obtained by using the RK ionization chamber and the SFD diode. Films have also been employed at a water equivalent depth of 5 cm in PMMA phantom.

The penumbra has been measured with diode also at the depth in water of 10 cm. In order to investigate the change in penumbra due to the asymmetric leaf setting, the profiles of four $1\times3\ \mathrm{cm}^2$ asymmetric fields have been measured at the depth of 1.5 cm in water, with the SFD detector at the isocenter plane. The field has been moved away from the central axis in the two orthogonal directions with steps of 1 cm, keeping the jaws open to $5\ \mathrm{cm}\times5\ \mathrm{cm}$.

G. Tissue maximum ratio

TMRs (tissue maximum ratios) have been derived from percent depth dose (PDD) measured in a water tank with different detectors moved within the tank by the RFA300 (Scanditronix) software. The PDD have been acquired for field sizes from 1×1 to $9\times9\ \mathrm{cm}^2$ with a source to phantom surface distance of 98.5 cm; the RK cylindrical ionization chamber and the silicon SFD diode were used. TMRs have been calculated for 1×1 to $9\times9\ \mathrm{cm}^2$ field size using the method described in Ref. 8, which takes into account the ratio of the phantom scatter factors. The results of TMRs calculated with and without this correction are reported in literature:[9] they show no difference in the TMR curve for a 40-mm-diameter circular beam and a maximum difference less than 2% at depths larger than 10 cm for a 12.5-mm-diam circular beam. No correction has been applied for the ratio in this work for the field $1\times1\ \mathrm{cm}^2$.

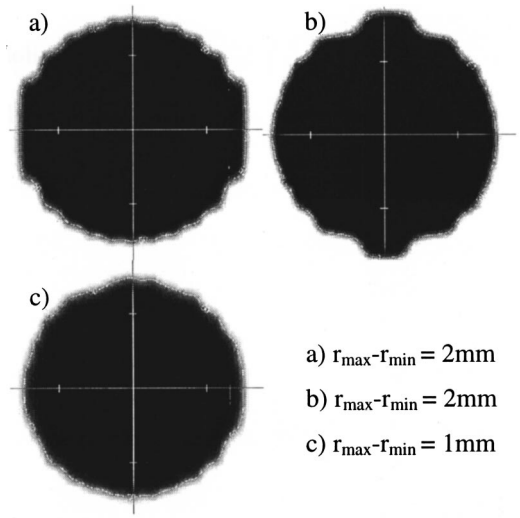

FIG. 4. Circular 3-cm-diam field obtained (a) with the lower level of leaves; (b) using the upper level of leaves; (c) by all leaf banks. The 50% isodose lines are displayed and the differences between maximum and minimum distances from field center to 50% isodose line are reported.

III. RESULTS AND DISCUSSION

A. Field shaping

The feature that is unique to this collimator is the availability of four leaf banks, so that the conformation is obtained in the two orthogonal directions and it is more accurate. This statement is supported by the analysis of some particular configurations that have been realized. As shown in Fig. 4, a 3-cm-diam circular field has been shaped in three different ways: (1) using only the lower level of leaves, (2) using only the upper level, (3) by all the leaf banks. The differences between maximum and minimum distances from field center to 50% isodose line are 2, 2, and 1 mm, respectively, for the three cases. The resulting values indicate the improvement in the conformation when both leaf levels are used. Even more, there are some field shapes which can be obtained only with a bi-directional collimator; an example of this peculiarity is the four-lobe shape shown in Fig. 5.

B. Output factors

The output factors measured with the PTW Pin Point ionization chamber are plotted in Fig. 6. As expected, the values obtained with the jaws opening following the aperture of the leaves are lower than the ones with fixed opening of the jaws, due to more head scattering with large jaw opening. Moreover, they are about 1% higher than the corresponding data measured without μMLC: the small difference is due to the scatter contribution from the leaf banks. The output be-

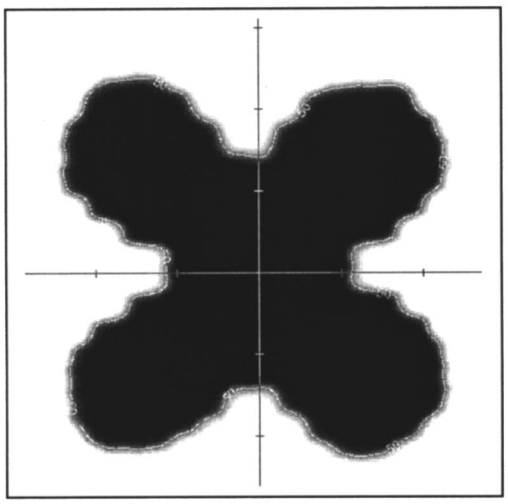

FIG. 5. Example of a field configuration that can be shaped only with a bi-directional collimator.

havior observed with the jaws open at 10 cm×10 cm field is due above all to the increase of the phantom scatter with the field size with some scatter contribution from the μMLC.

Figure 7 shows the comparison between measurements performed with different detectors at the depth of 1.5 cm in water, always keeping the jaws open to 10 cm×10 cm. Data have been normalized to a 10×10 cm^2 field shaped by jaws, without the μMLC.

For field size larger than 2×2 cm^2 the maximum difference between the values measured with all the employed detectors is about 1.5%; moreover the results obtained with the silicon diode are always lower than the values measured with the ionization chambers. Because of the higher absorption coefficient in silicon for low energy photons as compared with water, there is a significant over-response for the diode in large fields due to the increased number of low energy scattered photons. Since the contribution of scattered photons is lower in small fields, the output factors for these field sizes measured with the semiconductor detector are underestimated with respect to the ionization chamber values. Otherwise, the lateral electron equilibrium is maintained in narrow fields for diode while it is degraded for the ionization chamber. In fact, the range in silicon is shorter than in water resulting in a slower decrease of the electron fluence compared with the water equivalent detector when the field size decreases.[1] These two mentioned effects partially counteract explaining the agreement in the experimental results between the two kinds of detectors.

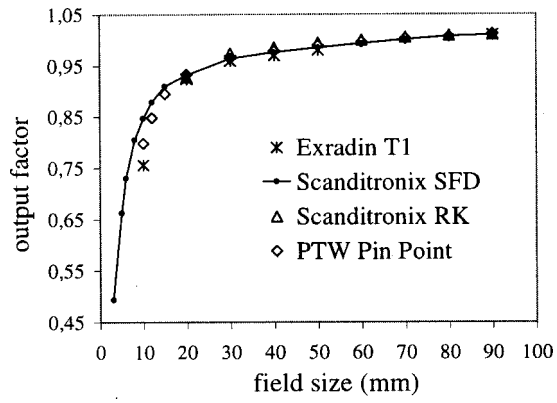

FIG. 7. Comparison between measurements performed with different detectors at depth of 1.5 cm in water.

For field size less than 2×2 cm^2 the RK chamber has not been used because of the length of its cavity, too long if compared with the field size. The Exradin T1 chamber has a lower cavity length, but anyhow the measured value may be underestimated due to the volume averaging effect. In fact, the beam is expected to be nonuniform over the spatial extent of the detector. This effect should be lower for the Pin Point chamber, but still relevant considering its cavity length of 5 mm: for the 1×1 cm^2 field size, the discrepancy between the SFD and the Pin Point chamber is about 5%. The elevated disagreement can be explained considering not only the problems already mentioned, but also the critical conditions for the detector positioning. For field sizes even smaller only SFD diode has been employed, owing to its smaller sensitive volume.

In Fig. 8 the agreement among the output factors obtained at a depth of 5 cm, with all the previous detectors and also the TLDs, is reported. The behavior of the detectors is simi-

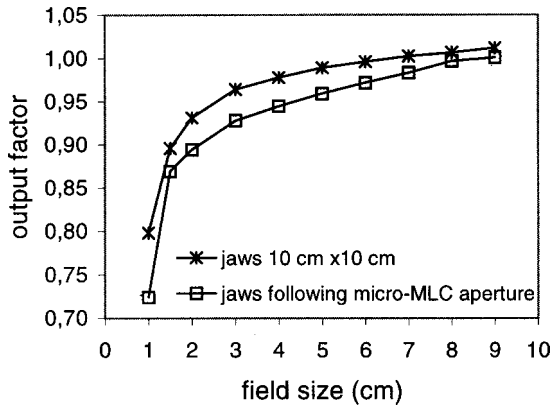

FIG. 6. Output factors measured in water at depth of maximum dose, for two jaw settings, with Pin Point chamber.

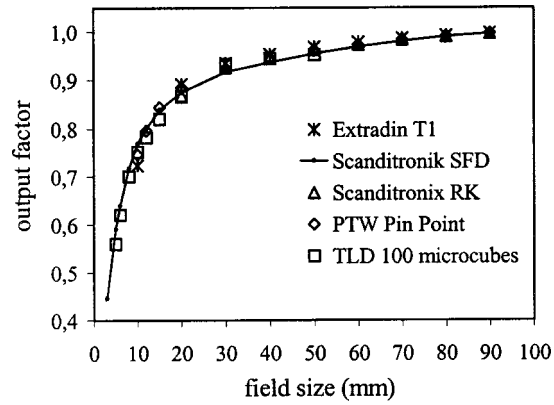

FIG. 8. Comparison between measurements performed with different detectors at depth of 5 cm in water.

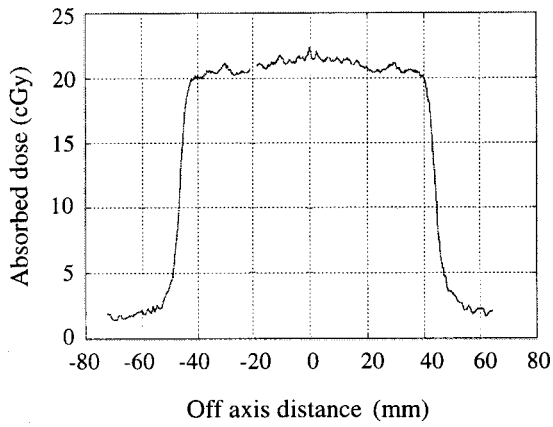

FIG. 9. Transverse dose profiles under one bank of leaves. The profile is scanned perpendicular to the direction of the leaf traveling. The central axis absorbed dose for the open field (5 cm×5 cm) is 460 cGy.

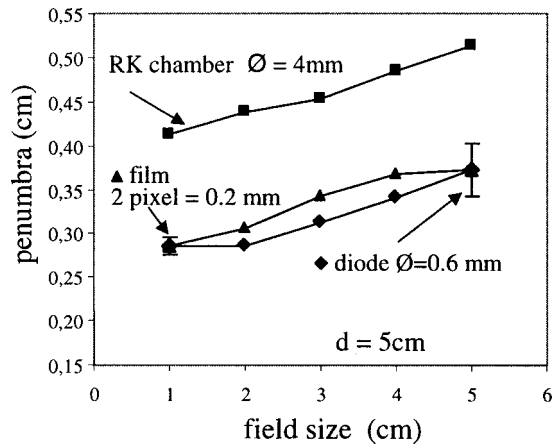

FIG. 10. Penumbra behavior vs field size obtained with different detectors. The estimated uncertainties are reported as bars only for the film and the SFD diode.

lar to the previous one at the depth of the maximum dose. The thermoluminescent dosimeters supply data in agreement within 2% with the other detectors for field size greater than 2×2 cm^2. In the field size range 1–2 cm the same agreement holds among TLDs, Pin Point and SFD. For smaller field sizes the comparison is meaningful only between microcubes and diode, because all the ionization chamber output factor values are at some extent lowered by the averaging effect. The agreement is within 3% (i.e., within the TLD uncertainty) except for 5% with the 5 mm field size. Such a discrepancy can be justified considering the critical measurement conditions besides the detector uncertainties. The agreement among the different detectors is slightly better at the depth of 5 cm than at $d_{\max}$; this can be due to the change in the energy spectrum with the depth, in particular to the decrease in the contamination radiation.

For field size bigger than 2 cm we have decided to evaluate the output factor as the average values between the data measured by all the detectors. In the range 1–2 cm only Pin Point, SFD, and TLDs have been considered, while for smaller fields the only detectors employed are the SFD and the microcubes because of their elevated spatial resolution. We attribute to the resulting values an uncertainty of 2% (maximum difference between the average values and the measurements with different detectors), compatible with the complexity of experiments with small radiation fields.

C. Leakage and leaf transmission tests

Film dosimetry has been used for leakage and leaf transmission evaluation. The transmission under two jaws has been estimated to be lower than 0.05%, while the transmission under only one jaw is lower than 0.5%.

Transverse dose profiles have been measured closing one bank of leaves at a time. Each profile has been obtained along the direction perpendicular to the leaves' traveling. An example is reported in Fig. 9. The alternation of peaks and troughs in the distribution is, respectively, due to the leakage between adjacent leaves and transmission through each leaf. The profile is not regular enough to permit the quantification of the leakage and leaf transmission, anyhow the maximum leakage between leaves can be evaluated equal to 5%. Both banks of leaves show the same behavior. On both sides of the profile, about 3 cm far from the center, a shallow sinking can be observed: it is due to carbon bars in the μMLC device. This attenuation effect is about 1%, so that the presence of the bars is consistent with an accurate dose delivery.

With both levels of leaves fully closed, the measured transmission is about 0.4%.

The results obtained with film dosimetry have been exactly confirmed (within the meaningful digits) by measurements performed (in one point) in water phantom with the Farmer chamber. The low dose level we find under two orthogonal banks suggests to shape the fields keeping fixed the aperture of the linac jaws, and changing only the leaf configuration. As already observed in literature,[10] this choice is more convenient for the prediction of the output factors in-

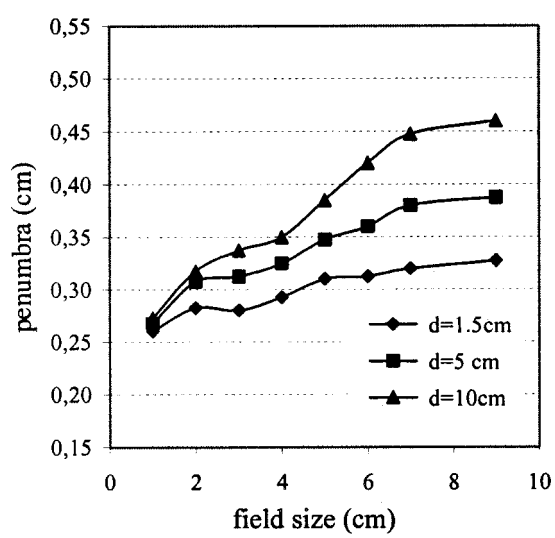

FIG. 11. Penumbra behavior vs field size at different depth in water. Measurements are performed with the SFD diode.

TABLE II. Penumbra values at the depth of 1.5 cm, measured by the SFD diode.

Field size (cm)	P_{20-80} (mm) Fields shaped by μMLC	Fields shaped by linac jaws
9	3.3	5.1
7	3.2	5.0
5	3.1	4.8
3	2.8	4.6

side the treatment planning system, because of the reduced dependence of the output on the field size.

D. Penumbra

The penumbra values have been measured in the in-line and cross-line directions. The difference between the corresponding results is always very small and anyhow lower than the uncertainty of the measurement (see the following). These findings agree with the setting of our collimator where, owning to the double leaf level, the radiation field is defined in both directions by the leaf ends so that leaf side effects do not affect penumbra. This feature of the device makes it favorably comparable also with double-focused miniature multileaf collimators.[10,11]

The penumbra parameter has been assumed the same in both directions, equal to the mean value.

The behaviors of the penumbra 20%–80% (P_{20-80}) as a function of the field size is reported in Fig. 10 for square fields. The experiments were performed with different detectors at the depth of 5 cm in water. The values range from 2.9 mm for the $1\times1\,\mathrm{cm}^2$ to 3.7 mm for the $5\times5\,\mathrm{cm}^2$ field, showing only slight increase with field size. A good agreement can be observed between the SFD diode and the film, while the RK chamber values are higher because of the large size of this detector. The uncertainties on the penumbra evaluated with the on-line dosimeters are due to the fact that the signal is averaged on the detector size, while the uncertainty on the positioning of the detector within the computerized water tank is negligible (reproducibility 0.1 mm). The uncertainties on the measurements performed with films can be evaluated to be about 200 μm, as discussed in Sec. II C.

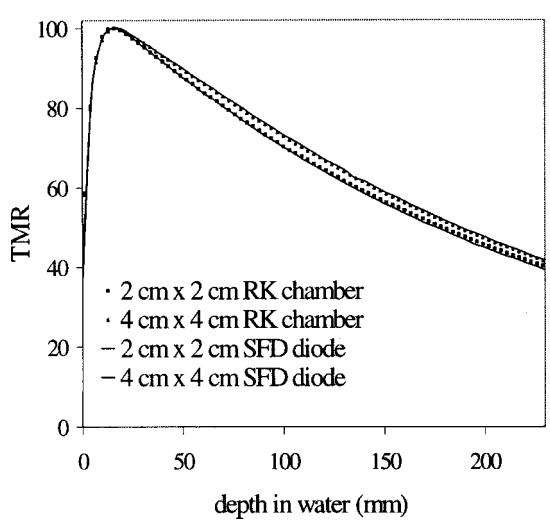

FIG. 12. Tissue maximum ratios derived from PDD measurements performed with SFD diode and RK chamber.

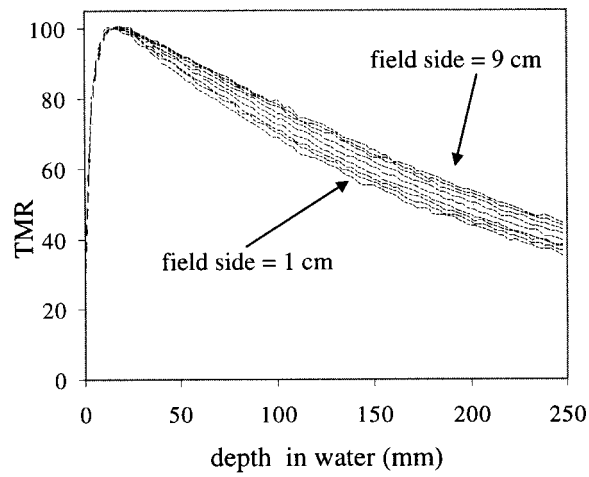

FIG. 13. TMR measured with the SFD detector for square field size increasing from 1 cm×1 cm to 9 cm×9 cm.

The dependence of the penumbra on depth is shown in Fig. 11: the P_{20-80} increases from $d_{\max}$ to the depth of 10 cm of 0.5 mm for the smallest field and of 1.3 mm for the largest one.

The penumbra value we input into the treatment planning system for each depth is equal to the value averaged both on field sizes and on the SFD diode and films responses.

In the penumbra study for $1\times3\,\mathrm{cm}^2$ asymmetric fields, we found that the variation of the effective field width (50%–50%) and penumbra values is negligible for the four investigated configurations (less than 0.4 mm).

Comparing the penumbra results with the value measured for the corresponding fields shaped by the linac jaws, without the μMLC, we observe a remarkable difference (Table II). This assessment agrees with the geometrical condition of the μMLC, which is closer to the patient than the jaws, but also implies a shaping of the leaves appropriated in order to minimize leaf end effects on the penumbra.

E. TMR tests

Tissue maximum ratios have been derived from PDD measurements performed with both stereotactic diode and RK ionization chamber. When the shift for the effective point of measurement for the RK chamber is taken into account, the agreement between the two sets of data is always within 2% at every depth and for each field size. As an example, data relative to 2×2 and $4\times4\,\mathrm{cm}^2$ fields are reported in Fig. 12. In Fig. 13 TMR curves are reported for all the investigated field sizes.

IV. CONCLUSIONS

In this work the complete characterization of the Acculeaf micromultileaf device has been carried out. Measurements

have been performed with the double aim of checking the quality of the equipment, applied for the first time in radiotherapy, and obtaining the parameters necessary for the determination of the dose to the patient.

The dosimetric study concerns the beam output as a function of the field dimensions, the transmission under and between the leaves, the depth dose distribution along the beam axis and the dose profiles in transverse planes.

The main problems related to this kind of experiment, that is the steep dose gradients and the possible lack of lateral electronic equilibrium in such small fields, have suggested the employment of different type of detectors.

Air-filled ionization chambers, the best tools to determinate the absorbed dose, need uniform particle fluence on the detector sizes. This requirement is not always verified because of the not flat profile of the smallest fields. In order to face this condition a silicon diode, planned for stereotactic fields, has been employed thanks to its better spatial resolution. Nevertheless silicon is not water equivalent material and the features of the dosimeter prevent the ''small cavity'' conditions from being verified.

Radiographic films, useful to perform spatial dose distributions, do not allow the accuracy necessary for the dose evaluation, due to large uncertainty associated with film dosimetry. Even in the case of LiF dosimetry, which permits high spatial resolution, the global uncertainty is rather large.

The mentioned critical points affect the measurements with ionization chambers, silicon diodes, TLDs, and radiographic films in a different way. Nevertheless, the obtained results are in a reasonable agreement among them.

The analysis of the performed experiments shows the following.

(1) The collimator is suitable for clinical use. In fact, the transmission under the two-leaf groups is the same as for a conventional jaw and the leakage between adjacent leaves does not introduce a significant contribution. In practice, the transmissions between and under the leaves are almost the same. Even more, we have to recall that the device gives a maximum spatial resolution (effective μMLC leaf width) at the isocenter of about 2.6 mm, so allowing an optimal field shaping.

(2) The penumbra is sufficiently small for all the measured configurations and it changes slowly with the field dimensions. The penumbra is also slowly increasing with the depth in water.

(3) SFD microdiode is suitable for measuring depth dose curves, in fact it supplies results in good agreement with RK chamber data. This assessment is of main concern, considering the higher user friendless of the diode, for which the correction for the effective point of measurement is not necessary. The measured depth dose curves are consistent with data reported in literature for small field sizes.[2,3,12]

(4) The output factors measured with all the detector employed are in a good agreement among them for square fields with size$\geqslant$2 cm. On the contrary, for smaller fields the agreement gets worse; in the field size range 2–1 cm the agreement is reasonable among SFD diode, Pin Point chamber, and microcubes while for field dimensions$\leqslant$1 cm only the diode and TL results can be considered reliable.

From our study, we can assess that the Acculeaf collimator is suitable for clinical use and the measured parameters can be employed as input data for the algorithms necessary to calculate the dose in the patient.

ACKNOWLEDGMENT

The authors wish to thank Ori Kanner, Chief Technology Officer of Alayna Enterprises Corporation, for his cooperation during the entire work.

[a]Author to whom all correspondence should be addressed at: Università di Firenze, Dipartimento di Fisiopatologia Clinica, Viale Morgagni 85, 50134 Firenze, Italia; electronic mail: marta@dfc.unifi.it

[1] M. Westermark, J. Arndt, B. Nilsson, and A. Brahme, ''Comparative dosimetry in narrow high-energy photon beams,'' Phys. Med. Biol. **45**, 685–702 (2000).

[2] R. K. Rice, J. L. Hansen, G. K. Svensson, and R. L. Siddon, ''Measurements of dose distributions in small beams of 6 MV x-rays,'' Phys. Med. Biol. **32**, 1087–1092 (1987).

[3] B. E. Bjärngard, J. S. Tsai, and R. K. Rice, ''Doses on the central axes of narrow 6-MV x-ray beams,'' Med. Phys. **17**, 794–799 (1990).

[4] P. Francescon, S. Cora, C. Cavedon, P. Scalchi, S. Reccanello, and F. Colombo, ''Use of a new type of radiochromic film, a new parallel-plate micro-chamber, MOSFETs, and TLD 800 microcubes in the dosimetry of small beams,'' Med. Phys. **25**, 503–511 (1998).

[5] J. L. Robar and B. G. Clark, ''A practical technique for verification of three-dimensional conformal dose distributions in stereotactic radiosurgery,'' Med. Phys. **27**, 978–987 (2000).

[6] J. L. Robar and B. G. Clark, ''The use of radiographic film for linear accelerator stereotactic radiosurgical dosimetry,'' Med. Phys. **26**, 2144–2150 (1999).

[7] S. E. Burch, K. J. Kearfott, J. H. Trueblood, W. C. Sheils, J. I. Yeo, and K. C. Wang, ''A new approach to film dosimetry for high energy photon beams: Lateral scatter filtering,'' Med. Phys. **24**, 775–783 (1997).

[8] *Central Axis Depth Dose Data for Use in Radiotherapy*, Supplement 25 (British Institute of Radiology, London, 1996).

[9] C. McKerracher and D. I. Thhwaites, ''Assessment of new small-field detectors against standard field detectors for practical stereotactic beam data acquisition,'' Phys. Med. Biol. **44**, 2143–2160 (1999).

[10] S. L. Meeks, F. J. Bova, S. Kim, W. A. Tomé, J. M. Buatti, and W. A. Friedman, ''Dosimetric characteristics of a double-focused miniature multileaf collimator,'' Med. Phys. **26**, 729–733 (1999).

[11] V. P. Cosgrove, U. Jahn, M. Pfaender, S. Bauer, V. Budach, and R. E. Wurm, ''Commissioning of a micromulti-leaf collimator and planning system for stereotactic radiosurgery,'' Radiother. Oncol. **50**, 325–336 (1999).

[12] C. F. Serago, P. V. Houdek, G. H. Hartmann, D. S. Saini, M. E. Serago, and A. Kaydee, ''Tissue maximum ratios (and other parameters) of small circular 4, 6, 10, 15 and 24 MV x-ray beams for radiosurgery,'' Phys. Med. Biol. **37**, 1943–1956 (1992).